# Concentration Dependence of Variability in Growth Rates of Microtubules

Susan Pedigo* and Robley C. Williams, Jr.†

*Department of Chemistry and Biochemistry, University of Mississippi, University, Mississippi 38677, and †Department of Biological Sciences, Vanderbilt University, Nashville, Tennessee 37235 USA

ABSTRACT Growth and shortening of microtubules in the course of their polymerization and depolymerization have previously been observed to occur at variable rates. To gain insight into the meaning of this prominent variability, we studied the way in which its magnitude depends on the growth rate of experimentally observed and computer-simulated microtubules. The dynamic properties of plus-ended microtubules nucleated by pieces of *Chlamydomonas* flagellar axonemes were observed in real time by video-enhanced differential interference contrast light microscopy at differing tubulin concentrations. By means of a Monte Carlo algorithm, populations of microtubules were simulated that had similar growth and dynamic properties to the experimentally observed microtubules. By comparison of the experimentally observed and computer-simulated populations of microtubules, we found that 1) individual microtubules displayed an intrinsic variability that did not change as the rate of growth for a population increased, and 2) the variability was approximately fivefold greater than predicted by a simple model of subunit addition and loss. The model used to simulate microtubule growth has no provision for incorporation of lattice defects of any type, nor sophisticated geometry of the growing end. Thus, these as well as uncontrolled experimental variables were eliminated as causes for the prominent variability.

## GLOSSARY

| | |
|---|---|
| $c$ | concentration of tubulin |
| $i$ | individual datum in a designated region of growth or shortening |
| $j$ | counter variable that represents an individual microtubule |
| $L$ | number of individual data points in the window used to determine rate of growth or shortening |
| $n$ | number of subunits added in a time interval |
| $N$ | total number of points in a growth interval for all growth intervals in a population |
| $Q$ | intrinsic variability |
| $r$ | average rate of growth or shortening |
| $r_i$ | rate of growth or shortening at datum $i$ |
| $dn/dt$ | average rate of growth or shortening in units of subunits/second |
| $\sigma$ | standard deviation in the rate of growth or shortening for a large data set |
| $s$ | standard deviation in the rate of growth or shortening for a small data set |
| $T$ | sampling frequency |
| Var($r$) | variance in the rate of growth or shortening |

## INTRODUCTION

In the presence of tubulin and GTP, microtubules undergo long excursions of growth and shortening, a process termed dynamic instability (Mitchison and Kirschner, 1984; Horio and Hotani, 1986; Walker et al., 1988; Erickson and O'Brien, 1992; Bayley et al., 1994). Growth of microtubules occurs through the addition of GTP- containing tubulin $\alpha\beta$-dimers. Hydrolysis of the E-site GTP, on the $\beta$-subunit, occurs sometime after the subunit is added, and so leaves a small cap of GTP subunits, or of GDP-$P_i$ subunits (Carlier and Pantaloni, 1981; Melki et al., 1996), at the growing end. The presence of the cap stabilizes the otherwise unstable body of the microtubule and provides a site for continued growth. Loss of the cap exposes the GDP subunits of the microtubule body and leads to rapid depolymerization. Because loss and recovery of the cap are rare events, large excursions in length occur, often amounting to several microns (many thousands of subunits) in length. Measurements of rates of growth and shortening of individual microtubules during these excursions have shown the rates of growth and shortening to be unexpectedly variable, both in vitro (Gildersleeve et al., 1992; Drechsel et al., 1992; Gamblin and Williams, 1995; Chrétien et al., 1995) and in vivo (Shelden and Wadsworth, 1993; Dhamodharan and Wadsworth, 1995; Rodionov and Borisy, 1997). At a constant concentration of tubulin, the rate of growth of microtubules (0.5-$\mu$m-long segments of microtubule, which contain ~800 subunits) can vary several-fold, even though the variability in rate expected from a simple Poisson model of the process would be only a few percent. Not only do

*Submitted October 26, 2001, and accepted for publication June 19, 2002.*

Address reprint requests to Dr. Susan Pedigo, Department of Chemistry and Biochemistry, University of Mississippi, University, MS 38677. Tel.: 662-915-5328; Fax: 662-915-7300; E-mail: spedigo@olemiss.edu.



0006-3495/02/10/1809/11 $2.00

neighboring microtubules differ in their growth rates at a particular time, but each single microtubule can also exhibit different growth rates at different times. Rates of shortening are similarly variable. This variability reveals complexity in the mechanism of dynamic instability.

Investigation of the underlying cause of variability has ruled out several possibilities. It is not an artifact of nucleotide depletion or of gross heterogeneity of the protein (Gildersleeve et al., 1992). It is not due to inadequate diffusion of tubulin monomers to or from the microtubule's growing or shortening end (Odde, 1997). Although variability can be modulated by microtubule-associated proteins (Drubin and Kirschner, 1986; Bré and Karsenti, 1990; Pryer et al., 1992; Drechsel et al., 1992; Kowalski and Williams, 1993a; Panda et al., 1995; Gamblin et al., 1996; Goode et al., 1997), it is not caused by them. Rather, it is an intrinsic property of the microtubule's body and cap (Billger et al., 1996; Odde, 1997), and characteristic of microtubules of several species (Billger et al., 1994).

### Possible causes of variation of rates

There are a number of possible causes for variability in rates of growth. One would expect that structural variations in the microtubule lattice could cause variations in rates of addition and loss of subunits. Variability could be caused by irregular geometry of the end of a microtubule, by irregular numbers of protofilaments in the cross section such as those seen by Chrétien et al. (1992), or by complex rules for addition of subunits to the end of the microtubule that involve GTP hydrolysis and associated conformational changes. Electron microscopic data, because of their snapshot nature, do not address the question of whether the boundaries separating 13-protofilament segments of microtubule from those with 14 protofilaments are stationary or mobile with respect to their position on the microtubule, or whether they are permanent or transient. Mobile or transient defects might be subject to annealing with the passage of time. Experiments of Gildersleeve et al. (1992), which sought a correlation between growth rates and shortening rates at particular points on the microtubule, led to the conclusion that if structural imperfections cause variability of rates, they must either be mobile or decay in a time that is short with respect to the lifetime (a few minutes) of a microtubule. It is thus unlikely that if variations in rates of growth and shortening are caused by irregularities, that they are both stationary and permanent. It is also important to note that because the mechanisms for growth and shortening differ from each other, so may the causes for variability in those processes.

We would expect that if lattice defects were the cause for variability that 1) the variability would increase with the rate of growth because more defects would be incorporated, and 2) populations of computer-simulated microtubules without defects would not demonstrate the same concentration dependence in the growth rate. In this paper, we report detailed studies of dynamic instability as a function of tubulin concentration, pooling data from a group of observations large enough to provide statistically meaningful measurements of variability. These studies show that in the experimentally observable range of tubulin concentrations, the intrinsic variability of growth and shortening rates remains nearly constant as the growth rate for a population increases. In addition, these studies show that the variability is approximately fivefold greater than predicted from a simple model of subunit addition and loss. Finally, they show that the phenomenon can be modeled in computer simulations of microtubule dynamic instability that allow only simple longitudinal and lateral microtubule lattice interactions and cooperative binding of subunits. It appears from these studies that variability in growth rates results from fundamental kinetic and equilibrium principles of lattice interactions in the microtubule and not from trivial experimental issues, complex geometrical and hydrolysis rules, or from incorporation of imperfections into the microtubule lattice.

## MATERIALS AND METHODS

### Reagents

PIPES was purchased from Boehringer Mannheim (Indianapolis, IN). GTP was purchased from Sigma Chemical Co. (St. Louis, MO). All microtubule assembly experiments were carried out in PEMD buffer (0.1 M PIPES, pH 6.9, 2 mM $MgSO_4$, 2 mM dithioerythritol, 2 mM EGTA, and 2 mM GTP).

### Tubulin and *Chlamydomonas* flagellar axonemal pieces

Microtubule protein was prepared from bovine brain by three cycles of temperature-dependent assembly/disassembly (Williams and Lee, 1982). Tubulin was purified from microtubule protein by chromatography on phosphocellulose (Williams and Lee, 1982; Correia et al., 1987). The purified tubulin was frozen drop-wise in liquid nitrogen and stored at −70°C. The tubulin was judged to be greater than 98% pure by Coomassie-blue-stained SDS-polyacrylamide gel electrophoresis.

For reproducibility of results, tubulin was submitted to a fourth cycle of assembly/disassembly as follows. A 500-$\mu$l sample of frozen tubulin solution (~2 mg of protein) was thawed rapidly at 37°C and then centrifuged for 10 min at 4°C in a Beckman TL-100 centrifuge at 55,000 rpm. The supernatant was mixed with an equal volume of PEMD in 8 M glycerol, brought to 2 mM GTP, and incubated at 37°C for 10 min to allow the assembly of microtubules, which were then pelleted at 34,000 rpm in the TL-100 for 10 min at 37°C. The pellet was disassembled by addition of 500 $\mu$l of cold PEM (0.1 M PIPES, pH 6.9, 2 mM $MgSO_4$, 2 mM EGTA, and 0.1 mM GTP) followed by a 10-min incubation, with stirring, on ice, and then centrifuged at 34,000 rpm in the TL-100 for 10 min at 4°C to pellet material that did not disassemble. The supernatant was gel-filtered into PEM by use of a NAP-5 column (Pharmacia, Uppsala, Sweden). Recovery was ~60%. Concentration of this tubulin stock was quantitated by a Bradford (1976) assay standardized against tubulin, the concentration of which had been determined spectrophotometrically from its $\epsilon_{278} = 1.20$ ml/(mg cm) (Detrich and Williams, 1978). It was brought to 2 mM dithioerythritol and 2 mM GTP and kept on ice. After dilution, the concentration was confirmed with a second Bradford assay. In general, the

precision of the Bradford assay was ±1 μM, and its accuracy was checked spectrally at regular intervals. In statistical analyses of results, the tubulin concentration was assumed to be known exactly.

*Chlamydomonas* flagellar axonemal pieces were isolated by the dibucaine-HCl method (Witman, 1986) from *Chlamydomonas reinhardtii* strain CC-125 and prepared as described previously (Gamblin and Williams, 1995). Pelleted axonemal pieces were suspended in PEMD, divided into 5-μl aliquots, frozen in liquid nitrogen, and stored at −70°C until needed. An experiment was performed to determine whether the axonemal pieces contained GTPase activity. None was observed after 30 min at 37°C (data not shown).

## Light microscopy

Microtubules were visualized by video-enhanced differential interference contrast light microscopy with a Zeiss Axiovert 35 microscope maintained at 37°C. Images were processed by the use of a Hamamatsu Argus-10 and recorded on a Mitsubishi Super-VHS videocassette recorder (Schnapp, 1986; Williams, 1992). Slides and coverslips were cleaned by sonication in a 1% Micro (Cole-Parmer Instrument Co., Chicago, IL) solution for 45 min, rinsed in copious amounts of doubly distilled water, and air dried. Reaction chambers were prepared with Parafilm spacers as described previously (Williams, 1992). Chamber volumes were ~20 μl, with depths of ~50 μm.

Microscope samples were prepared by introducing a 20-μl aliquot of the suspension of axonemal pieces into the chamber, inverting it, and allowing the axonemal pieces to settle and adhere to the coverslip for ~2 min at room temperature. To saturate the walls of the chamber with tubulin and thus to assure that the concentration was not diminished by adsorption, the chamber was rinsed with four successive 20-μl aliquots of the tubulin solution before the final 20-μl aliquot was introduced. The last aliquot was sealed in the chamber with Vaseline/lanolin/paraffin (1:1:1). Preparations were observed and recorded on videotape for no more than 50 min. We observed a tubulin-concentration-dependent increase in the mean number of microtubules nucleated per axoneme at both ends, as has been reported by others (Mitchison and Kirschner, 1984; Bré and Karsenti, 1990).

## Data analysis

Videotaped images of plus-end microtubules, which were distinguished from minus-end microtubules by the distinct morphology of the ends of *Chlamydomonas* flagellar axonemal pieces (Gamblin and Williams, 1995), were measured at intervals of 2.5–4.7 s by means of the computer program described by Gamblin et al. (1996). Length-versus-time data were then analyzed by a second computer program to determine rates of growth and frequencies of catastrophes and rescues (Gamblin et al., 1996). Shortening rates were determined in a separate analysis by review of the videotaped shortening events at each concentration of tubulin at half speed. This allowed an increase in the number of data points that could be measured during a shortening event while avoiding the difficulty in seeing the microtubule ends that occurs when tapes are viewed frame by frame. Only those shortening events longer than 5 μm were included in the shortening rate determination. The mean growth rates and shortening rates, $r^g$ and $r^s$, respectively, were calculated according to:

$$\langle r^g \rangle = [\Sigma r_i/N]_{\text{growth}} \quad \text{and} \quad \langle r^s \rangle = [\Sigma r_i/N]_{\text{shortening}}, \quad (1)$$

where $r_i$ is the rate corresponding to each data point within a growth or shortening event, $N$ is the number of all such points for the entire population, and the sum is taken over $1 < i < N$. The value of rate at each data point, $r_i$, was calculated as an average rate over an 11-data-point window ($i$th datum ± 5 data) as described by Gamblin et al. (1996). Growth rates were fitted to an equation of Walker et al. (1988), with the use of their notation for the rate constants:

$$\langle r^g \rangle = k_2^{e+}[\text{Tb}] - k_{-1}^{e+} \quad (2)$$

where [Tb] is the molar concentration of tubulin dimer, $k_2^{e+}$ is the second-order (pseudo-first-order) rate constant for the addition of subunits to (+) ends, and $k_{-1}^{e+}$ is the first-order (pseudo-zero-order) rate constant for loss of subunits from the (+) ends during the growth phase of microtubule dynamics. (The average rate of growth ($r^g$) and shortening ($r^s$) will be designated subsequently as $r$.)

The number of catastrophes occurring per unit time or per unit length of growth was determined by dividing the number of catastrophes in a single population by the total time in minutes or the total length in microns that the population spent in the growth phase. Rescues were treated equivalently. The uncertainty in these frequency measurements was estimated by dividing the square root of the number of events by the time or length spent in the growth phase. A control experiment was performed to determine the error (±0.13 μm) associated with measuring a stationary object on the video screen.

The standard deviation in the rates of growth for the populations of microtubules, although caused mostly by actual variation in rates, is also due in part to measurement error. To estimate the magnitude of that part, we used an algorithm by Morrison (1969) in which the random error of the rate is given by:

$$\text{Var}(r)_{\text{ran}} = \sigma_v^2/T^2[12/((L+2)(L+1)L)], \quad (3)$$

where $\text{Var}(r)_{\text{ran}}$ is the variance in the rate due to random measurement error, $\sigma_v^2$ is the observation error (±0.13 μm; Gildersleeve et al., 1992), T is the sampling frequency, and $L$ is the size of the window over which rate data were determined ($L = 11$ points; Gamblin and Williams, 1995).

## Simulations of microtubule dynamics

Simulations of microtubule dynamics were done by means of a Monte Carlo algorithm based on the lateral cap model of Bayley and colleagues (Martin et al., 1993; Bayley et al., 1990), written in-house. Monte Carlo simulations of microtubule growth suffer from simplistic treatment of complex phenomenon such as inhomogeneous diffusion. However, despite the limitations of a nondynamical method such as Monte Carlo to simulate kinetic phenomena, these simulations provide pseudo-dynamical parameters that are interesting to compare with parameters obtained from experimentally monitored microtubules. The lateral cap model provides for the following restrictions in the Monte Carlo simulations. Single subunits are added to or lost from the end of each of the 13 protofilaments. Only the ultimate tubulin subunit of each protofilament contains GTP on its β-subunit. All other subunits of each protofilament have hydrolyzed their E-site GTP to GDP + $P_i$. Thus, the addition of a subunit is coupled to hydrolysis of the E-site GTP of the previous subunit. Both intra- and inter-protofilament contacts are required for a subunit to add (longitudinal and lateral interactions, respectively). The strengths of these lateral and longitudinal interactions are adjustable parameters in this model and govern the rate of the dissociation events. Extensive calculations showed that more than one set of interaction constants resulted in simulated microtubule dynamics similar to those observed in vitro. In general, though, the rule for the choice of these constants was that the strength of interaction between the ultimate GTP-containing subunit for its neighbors was far greater than that of the GDP-containing subunits in the lattice. Using this model we simulated dynamics at the plus end of 13-protofilament B-lattice microtubules over a broad range of tubulin concentrations. For comparison with the data, a set of dissociation constants for the tubulin subunits was chosen that yielded dynamic behavior over a concentration range similar to that observed experimentally. Simulated data points were saved after every 500 iterations. Simulated length-versus-time data sets were then processed identi-

**TABLE 1 Dynamic instability parameters of experimentally observed microtubules**

| [Tb] ($\mu$M)* | $\langle r^g \rangle$ ($\mu$m/min)† | $Q_{gro}$ ($s^{-1}$)‡ | $\langle r^s \rangle$ ($\mu$m/min)§ | $Q_{sho}$ ($s^{-1}$) | $f_{res}$ ($min^{-1}$)¶ | $f_{cat}$ ($min^{-1}$)‖ | $Time_g$ (min)** | $Time_s$ (min)†† | Number of events gro‡‡ | Number of events sho§§ | $Q_{corr}$ ($s^{-1}$)¶¶ | Sec/pt | MT‖‖ |
|---|---|---|---|---|---|---|---|---|---|---|---|---|---|
| 16.6 | 1.69 ± 0.68 | 7.41 | −22.5 ± 11 | 146 | 1.48 | 0.52 | 62 | 21 | 45 | 38 (8) | 4.33 | 4.7 | 9 |
| 18.1 | 2.54 ± 0.84 | 7.64 | −30.9 ± 15 | 197 | 1.58 | 0.45 | 215 | 45 | 119 | 102 (18) | 3.59 | 2.9 | 34 |
| 20.7 | 2.82 ± 0.94 | 8.49 | −31.6 ± 22 | 415 | 2.19 | 0.34 | 53 | 8.7 | 30 | 21 (6) | 4.91 | 3.3 | 9 |
| 22.6 | 3.01 ± 0.91 | 7.45 | −32.8 ± 14 | 166 | 1.7 | 0.25 | 119 | 15 | 57 | 34 (9) | 4.28 | 3.4 | 27 |
| 26.2 | 3.68 ± 1.18 | 10.2 | −29.2 ± 11 | 112 | 2.07 | 0.12 | 92 | 5.8 | 31 | 12 (6) | 6.23 | 2.9 | 19 |
| 29 | 3.47 ± 0.92 | 6.61 | | | | | 70 | 0 | 13 | 0 | 3.93 | 3.5 | 13 |
| 35.4 | 5.40 ± 1.20 | 7.22 | | | | | 56 | 0 | 17 | 0 | 4.06 | 2.5 | 17 |

*Concentration of tubulin dimer.
†Growth rate of the population (see Eqs. 1 and 2), designated $V^{e+}$ by Walker *et al*. (1988).
‡Intrinsic variability, $Q$, is the variance in the rate divided by the rate, Eq. 4.
§Shortening rate of the population (Eq. 1), designated $V^{rs+}$ by Walker *et al*. (1988).
¶$f_{cat}$ is the number of catastrophes divided by the total time spent in a growth phase.
‖$f_{res}$ is the number of rescues divided by the total time spent in a shortening phase.
**Time spent in growth phase.
††Time spent in shortening phase.
‡‡Number of points observed during growth intervals. The number of growth events was determined by summing all growth regions regardless of whether they were punctuated by catastrophes and rescues.
§§Number of points observed during shortening intervals. The values in parentheses are the numbers of events at least 5 $\mu$m long.
¶¶Intrinsic variability, $Q$, corrected for measurement error (Eq. 3).
‖‖Number of microtubules in the population.

cally to the experimentally obtained data sets to enable comparison of theory with experiment. Data from simulated microtubules did not have random error due to measurement (see Eq. 3).

## RESULTS

### Overall dynamic instability characteristics

Extensive measurements of dynamic instability were made over a twofold range of tubulin concentration, which produced a greater than threefold change in growth rate. The population of microtubules at each tubulin concentration was analyzed to determine the dynamic instability parameters (i.e., rates of growth and shortening and frequencies of catastrophe and rescue) and their variability. Table 1 summarizes all parameters describing the dynamics of the experimental populations of microtubules. In accord with expectations and Eq. 2, mean growth rates increased linearly with the concentration of tubulin (slope = $k_2^{e+}$ = 0.17 ± 0.02 $\mu$m/min/$\mu$M (4.6 ± 0.5 subunits/(s $\mu$M)) and intercept = $k_{-1}^{e+}$ = 0.86 ± 0.53 $\mu$m/min (23 ± 14 subunits/s)). As also expected, shortening rates showed no appreciable concentration dependence. Catastrophes (stated either on a per-time basis or a per-length basis) became steadily more rare with increasing tubulin concentration. The frequency of rescue per time of shortening increased marginally with the tubulin concentration, whereas the frequency of rescue per length of shortening was independent of the concentration of tubulin. The data, taken together, show that these populations of microtubules behaved in a fashion consistent with expectations based on previous studies and are, therefore, a good system for examining the phenomenon of the concentration dependence of variability in rates of growth and shortening.

### Variability in dynamic instability characteristics

The large standard deviations in growth and shortening rates indicate that variability in the measured rates is large. As shown by Gildersleeve et al. (1992), it is variations in the actual rate of growth or shortening that make the chief contribution to this variability, whereas random measurement errors contribute comparatively little (see below). The aim of the present work is to discern how this actual variability is affected by the rate at which microtubules grow. Therefore, for simplicity in what follows, although changes in concentration were used to produce changes in rate, the data are plotted against the mean growth rate itself, instead of being plotted against the concentration.

Fig. 1 reveals how the variability in growth and shortening rates depends on the rate at which the microtubules grew. Fig. 1 *A* shows the growth-rate dependence of the standard deviation of the growth rate (○). It is clear that faster microtubule growth is associated with a larger standard deviation in growth rate. This sort of behavior would be expected from most mechanisms of growth that might be imagined. For this reason, the standard deviation by itself is not a very useful measure to distinguish between possible causes of variation. A better measure is the intrinsic variability of growth, $Q$:

$$Q = \mathrm{Var}(r)/\langle r \rangle, \quad (4)$$

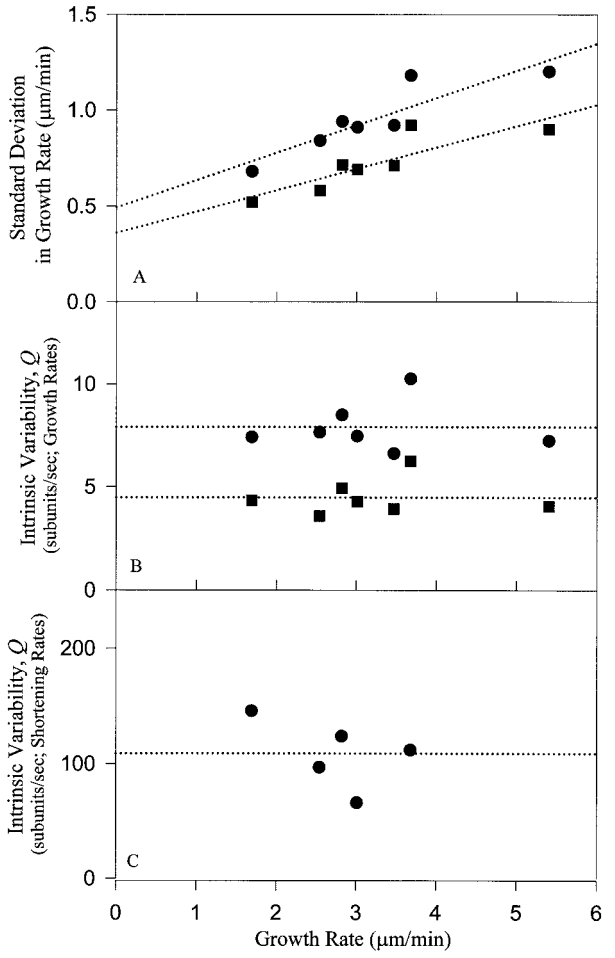


FIGURE 1 Variability of microtubule growth rates. (*A*) Standard deviation of the growth rate (●) as a function of the mean rate of growth of the microtubules. (The slope of the line is 0.142 ± 0.032; the intercept is 0.49 ± 0.11 μm/min.) Also shown is the standard deviation in the growth rate (■) corrected for measurement error according to Eq. 3. (*B*) The intrinsic variability in growth rate, $Q$ (●), plotted as a function of the mean growth rate of the microtubules. $Q$ is calculated using Eq. 4 with average rate and variance in rate calculated from measurements in units of subunits/second. The dashed line represents the mean of the data (7.9 ± 1.2 subunits/s). Also shown is the intrinsic variability corrected for measurement error as in *A* (■), where the dashed line is the mean of the data (4.5 ± 0.9 subunits/s). (*C*) The intrinsic variability in shortening rate as a function of the mean rate at which the microtubules grew. The mean of the data is 109 ± 30 subunits/s. In each case, the rates were measured in an 11-point moving window, as referenced in Materials and Methods, and all growth intervals in a population were equally weighted.

where Var($r$) (approximated in practice by the square of the standard deviation) is the variance in growth or shortening rate, given by:

$$\mathrm{Var}(r) = \sigma^2 = (1/N)\Sigma[(dn/dt)_i - \langle dn/dt\rangle]^2, \qquad (5)$$

where $\sigma$ is the standard deviation, $N$ is the number of rates in a population, $n$ is the number of subunits added to or lost from a microtubule in time interval $t$, and the indicated sum is taken over all $i$ from 1 to $N$. The value of $dn/dt$ is equivalent to $r$ but expressed in subunits per time rather than length per time.

Fig. 1 *B* shows measured values of $Q$ over the range of tubulin concentration explored experimentally. It is clear that $Q$ does not depend in a measurable way on the rate of microtubule growth in the experimentally accessible range of tubulin concentrations, even though the growth rate itself varied by approximately threefold. Fig. 1 *C* shows the relationship between the measured value of $Q$ in shortening and the rate at which the microtubules grew. (The numerical values for data are shown in Table 1.) The shortening data show no evidence that a microtubule that grew rapidly has any greater tendency to shorten in a variable way than does one that grew slowly.

Because there is finite and unavoidable observational error associated with these studies, we examined whether this error varied with concentration in a way that would change the conclusion of these studies. Equation 3 allows one to estimate the contribution to the variance from observational error and sampling frequency. It showed that the random error in the rate decreases with increasing sampling frequency. Despite an attempt to acquire the length data of the microtubules at equal time intervals, the actual time intervals varied by as much as a factor of 1.7 (see Table 1). Fig. 1 *A* shows the corrected standard deviation in the growth rate (■; standard deviation for the population minus the estimated standard deviation due to observational error) for each population plotted against the rate of growth for that population. One can see that the correction for observational error has decreased the value of the standard deviation for each population, but the trend in the data is unchanged (positive slope). Likewise, in Fig. 1 *B*, one can see that the absolute values for $Q$ have changed once the standard deviation is corrected for random error (Eq. 3; Fig. 1 *B*, ■) but that the concentration-independent trend of the data remains unchanged.

## Are some groups of microtubules more disperse than others?

To evaluate the dispersion between the mean rates for individual microtubules, the average rate of growth for each microtubule, ($r_j$), was calculated:

$$\langle r\rangle_j = \Sigma r_i/N_j, \qquad (6)$$

where $r_i$ is the growth rate corresponding to each data point in the $j$th microtubule, $N_j$ is the number of growth points in the $j$th microtubule, and the sum is taken over $1 \le i \le N_j$. The standard deviation in $r_j$ is given by:

$$s(\langle r\rangle_j) = \{[1/(N_j - 1)]\Sigma[r_i - \langle r\rangle_j]^2\}^{1/2} \qquad (7)$$

Fig. 2 shows these microtubule-specific means and standard deviations for a representative group, along with the mean and standard deviation of the group as a whole, as calculated

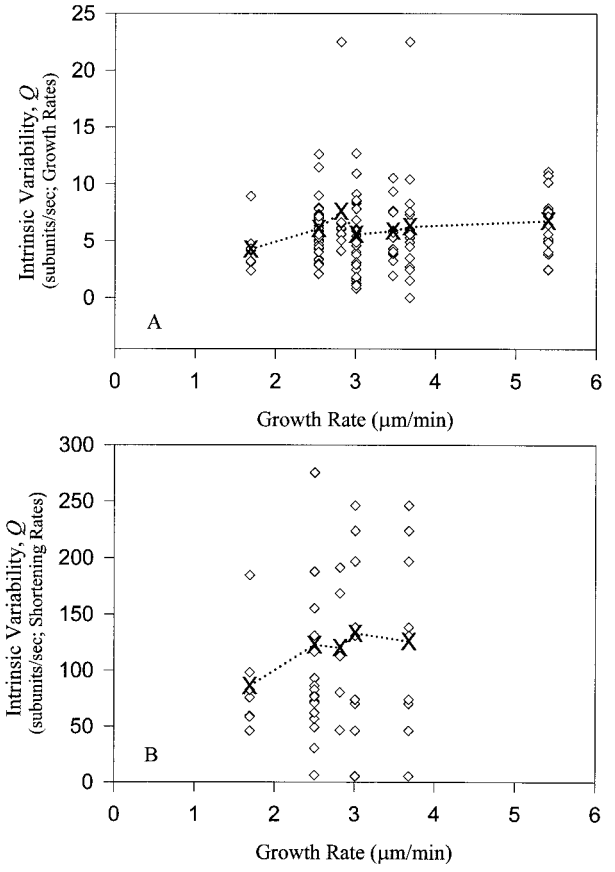


FIGURE 2 The intrinsic variability, $Q$, of growth rates ($A$) and shortening rates ($B$) for individual microtubules as a function of the rate at which they grew. The value of $Q$ calculated from Eq. 4, using Eqs. 6 and 7, for each microtubule is represented as a point ( $\diamond$ ). The average $Q$ value for each population is indicated by X. To guide the eye, a dotted line connects the average $Q$ values.

by Eqs. 1 and 5. The similarity of behavior of all the microtubules in the group is clear in this representation. Subpopulations are not evident.

## Are particular microtubules significantly more variable than others in the same group?

Fig. 3 shows graphically the dispersion of the variability of individual microtubules in each population. Each point represents the value of the mean intrinsic variability in growth rate, $Q$, for a particular microtubule observed at a particular concentration of tubulin. Against the background of normal overall behavior of the groups of microtubules, these data provide a sensitive means of detecting shifts in the distributions of possible subpopulations. They allow one to see, for instance, whether the overall statistics of Fig. 1 $B$ might mask the appearance at high concentration of a class of hypervariable microtubules balanced by a subpopulation of microtubules with very narrowly distributed growth rates. Evidently, this is not the case. To the contrary, the variabilities of the individual microtubules are dispersed smoothly and roughly equally on either side of the means, which are indicated by $\times$ in Fig. 2. This average intrinsic variability of growth and shortening rates does not change with the rate at which microtubules grew. The overall mean values are $Q = 6.0 \pm 1.0$ subunits/s for growth and $Q = 117 \pm 18$ subunits/s for shortening. These numbers reveal the shortening process to be much more variable than growth. The data in Figs. 2 and 3, taken as a whole, indicate that populations of more and less variable microtubules are not detectable.

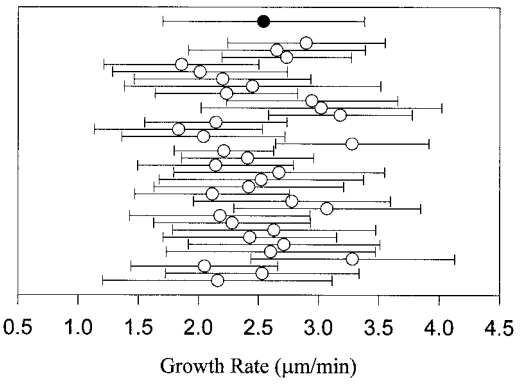


FIGURE 3 The average growth rate (Eq. 6; $r_j$ (○)) and standard deviation in the growth rate (Eq. 7; $s$ ($r_j$) (*error bars*)) for every microtubule in a representative population ([tubulin] = 18 $\mu$M) is shown ($r_j \pm \sigma$ ($r_j$)) along with the mean rate and standard deviation in that rate for the population as a whole ($r \pm \sigma$ ($r$); ●).

## Simulations of microtubule dynamics

To investigate whether the existing lateral-cap molecular model of microtubule dynamic instability can account in part for the observations, simulations were undertaken. Only simulated growth processes are reported here, because of the complex nature of shortening events (Mandelkow et al., 1991), which may not be accurately represented in the model. The dynamic instability parameters for the simulated microtubules are in Table 2. Over the range of concentration that was explored, the rate of growth for the simulated microtubule populations varied linearly with concentration of tubulin as defined by Eq. 2. The distributions of the growth rates simulated at each concentration are represented as one standard deviation from the mean growth rate. The frequencies of catastrophe ($min^{-1}$ of growth) decreased and of rescue ($min^{-1}$ of shortening) increased for simulated microtubules, consistent with the behavior of experimentally observed microtubules. Fig. 4 shows the intrinsic variability of those simulated microtubule populations for which dynamics was observed as a function of the rate of simulated growth. Values of $Q$ for simulated microtubules are similar to those experimentally observed ($6.8 \pm 0.6$ $s^{-1}$ simulated; $7.9 \pm 1.2$ $s^{-1}$ observed; cf. Fig. 1 $B$) and do not change systematically with the growth rate.

**TABLE 2 Dynamic instability parameters of computer-simulated microtubules**

| [Tb] ($\mu$M)* | $\langle r^g \rangle$ ($\mu$m/min)† | $Q_{gro}$ ($s^{-1}$)‡ | $f_{res}$ ($min^{-1}$)§ | $f_{cat}$ ($min^{-1}$)¶ |
|---|---|---|---|---|
| 24 | 1.84 ± 0.72 | 7.63 | — | — |
| 25 | 1.85 ± 0.70 | 7.17 | 4.02 | 2.68 |
| 26 | 2.02 ± 0.73 | 7.16 | 6.72 | 2.50 |
| 27 | 2.29 ± 0.73 | 6.37 | 7.11 | 1.63 |
| 28 | 2.65 ± 0.84 | 7.28 | 9.90 | 0.77 |
| 29 | 3.00 ± 0.84 | 6.30 | 20.2 | 0.36 |
| 32.5 | 3.29 ± 0.80 | 5.27 | 21.8 | 0.24 |

*Concentration of tubulin dimer.
†Growth rate of the population (see Eqs. 1 and 2), designated $V^{e+}$ by Walker *et al*. (1988).
‡Intrinsic variability, $Q$, is the variance in the rate divided by the rate, Eq. 4.
§$f_{res}$ is the number of rescues divided by the total time spent in a shortening phase.
¶$f_{cat}$ is the number of catastrophes divided by the total time spent in a growth phase.

## DISCUSSION

The experiments described above reveal the way in which the variation in rates of growth and shortening depends on the tubulin concentration and therefore on the rate of growth of the microtubules. The first main finding is that the intrinsic variability of growth rates, and that of shortening rates, does not increase with the rates themselves but remains effectively constant over the concentration range that is accessible experimentally. The second major finding is that the variability in growth and shortening rates does not result from differences between members of the population of microtubules: each microtubule is variable and all microtubules are statistically indistinguishable in their behavior.

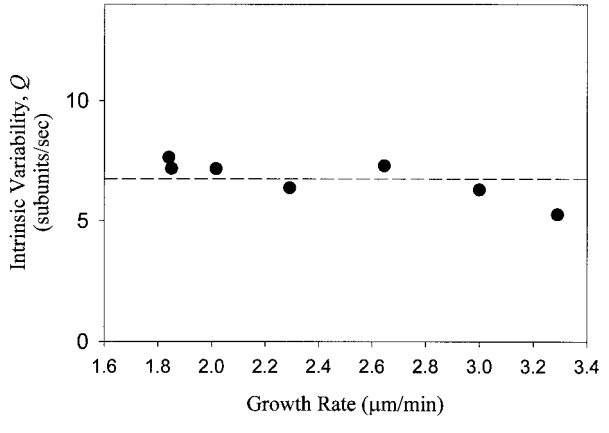


FIGURE 4 Intrinsic variability of computer-simulated microtubule populations as a function of growth rate for populations in which one can observe dynamic behavior experimentally. The dashed line is the average of the data points over this concentration range. Compare this figure directly with Fig. 1 *B*, which represents experimental data.

### Dynamics of single microtubules

In qualitative agreement with previous work (Walker et al., 1988; Chrétien et al., 1995; Pryer et al., 1992), the present data show that the mean rate of growth of individual microtubules increases with increasing tubulin concentration. The kinetic constants for the growth phase calculated from Eq. 4 are very similar to those for plus-end microtubules reported by Chrétien et al. (1995) and are slightly less than those determined for plus-end microtubules, but nearly identical to those determined for minus-end microtubules, by Walker et al. (1988). Shortening rates were independent of the tubulin concentration. The present value of 840 ± 220 subunits/s is in good agreement with those reported by Walker et al. (1988) (733 ± 23 (SEM) subunits/s for plus ends and 915 ± 72 subunits/s for minus ends), with Chrétien et al. (1995) (853 ± 184 subunits/s), and with Gamblin and Williams (1995) and Gildersleeve et al. (1992) (1000 ± 760 subunits/s). The quantitative differences between the rate constants measured here and those observed before are moderate given the differences in conditions (see review by Correia and Lobert, 2001). The data gathered here therefore appear to represent a typical population of microtubules formed in vitro from pure tubulin.

Consistent with the methods of other studies (Gildersleeve et al., 1992; Kowalski and Williams, 1993a,b; Gamblin and Williams, 1995; Gamblin et al., 1996), the data in Fig. 1, *B* and *C*, represent the variation in the pooled (or population-average) growth and shortening rates from all the microtubules measured at each concentration, without reference to particular microtubules. Because it pools all available rates, it embodies the assumption that all the microtubules in a population behave equivalently when observed over a long time. Treatment of the data in this manner is supported by Figs. 2 and 3, which demonstrate that the populations of microtubules are statistically uniform. Each individual microtubule in a population has an intrinsic variability associated with it. Fig. 2 shows that, as was true for the pooled data in Fig. 1, *B* and *C*, the average intrinsic variability for the individual microtubules is also independent of growth rate. In addition, the average intrinsic variability of rates for individual microtubules (6.0 ± 1.0 subunits/s; Fig. 2 *A*) is approximately equal to that for the population (7.9 ± 1.2 subunits/s; Fig. 1 *B*). The similarity also applies to shortening rates. The average intrinsic variability (117 ± 18 subunits/s; Fig. 2 *B*) is approximately equal to that for the pooled data (109 ± 30 subunits/s; Fig. 1 *C*). The magnitude of $Q$ reflected in the central findings (Fig. 1, *B* and *C*) is therefore determined largely by the intrinsic variability of individual microtubules over their lifetimes rather than differences between microtubules. This fact implies that measuring one microtubule for a long period is equivalent to monitoring many microtubules for a short period. Concern for the possible variability of microtubule dynamics arises from results in the literature. There

is strong circumstantial evidence to suggest that microtubules may exhibit functional differences from each other due to differences in isoform composition (Hoyle and Raff, 1990; Banerjee et al., 1992; Banerjee and Ludueña, 1992; Panda et al., 1994; Derry et al., 1997; reviewed by Ludueña, 1998) or due to structural differences, either short-lived or more permanent (Pierson et al., 1978; Chrétien and Fuller, 2000). Differences in functional properties observed in vivo can result from the presence of different isoforms in microtubules (Hutchens et al., 1997; reviewed by Wilson and Borisy, 1997).

### Interpretation of the intrinsic variability, *Q*

To allow interpretation of the variability observed over a wide range of rates of growth, we have measured (variance in the rate)/(mean value of the rate), called the intrinsic variability, denoted by $Q$, and given by Eq. 4. $Q$ is a useful measure of variation for the following reason. In ordinary models of polymer growth, subunits are added and removed at random at the end of the structure according to Eq. 2. Consider a single microtubule ($j$) observed at a large number of time intervals during growth phases (or a population of many equivalent microtubules observed simultaneously). In a particular time interval $(\delta t)_j$, suppose that a number of subunits $(\delta n)_j$ is added. The rate of growth during this interval is then given by $r_j$, where $r_j = \delta n_j/\delta t_j$ . If all time intervals are equal, then $r_j = (\delta n/\delta t)_j$. Simple Poisson fluctuations in the number of subunits added in a unit of time would yield a variance proportional to the mean value of the $r_j$, denoted $r$, for the group of observations (Oosawa, 1970; Dye and Williams, 1996):

$$\mathrm{Var}(r) = \langle r \rangle \tag{8}$$

Although it is not certain that such a simple model as Eq. 8 actually applies here (see below), it represents the simplest possibility with which to compare the data. Under these circumstances, the variance and the standard deviation, $\sigma$, would increase with growth rate, because:

$$\sigma = [\mathrm{Var}(r)]^{1/2} = \langle r \rangle^{1/2}, \tag{9}$$

whereas $Q = \mathrm{Var}(r)/r$ (Eq. 4) would remain constant and at a value of 1. The same principle holds for the addition/removal of oligomers.

The model for microtubule growth summarized in Eq. 2 reflects the assumed process of addition and loss of subunits occurring at random at the tip of a microtubule. For microtubules that are dynamic but in a growth phase, the complex issues of the GTP-cap and instability of the GDP-tubulin body of the microtubule intervene, and we might expect that the mechanism would be more complex. That this is the case is shown by the fact that experimental values of $Q$ are approximately fivefold greater than Eq. 8 predicts. Equations 2 and 8 would not apply to shortening microtubules, where the process is nonrandom and independent of tubulin concentration.

Similarly, Odde et al. (1996) noted variability in the growth rate several-fold larger than predicted by Poisson fluctuations in the addition and loss of subunits from the microtubule end or by measurement uncertainties. The magnitude of these contributors to the measured variability in rates is on the same order as that reported here and validates the correction for uncertainty in the data due to measurement (Fig. 1, *A* and *B*). However, although this correction for measurement uncertainties changes the magnitude of the value for the standard deviation and therefore $Q$, it does not change the conclusions drawn from these experiments. We observed a gradual slowing of growth rates for some microtubules before a catastrophe as discussed by Odde et al. (1995), but these data did not broaden the rate distribution significantly.

### Possible causes for variability that are excluded by the data

The apparent concentration independence of variability in rates of growth and shortening in Fig. 1 *B* argues strongly either that imperfections or defects in the lattice do not become more common at higher growth rates or that an annealing process by which they can be removed is rapid enough to keep up with the increased rate of subunit addition. In either case, variability of growth and shortening rates appears not to be caused by incorporation of irregularities into the microtubule lattice. This conclusion is supported by the data in Fig. 4 from simulated microtubules where lattice imperfections were not allowed by the model.

Another unlikely cause for the intrinsic variability in rates is that there may be a fraction of conformationally compromised, or dead, tubulin that is incorporated into the microtubule lattice, possibly blocking the end momentarily. If such compromised tubulin (Tb*) associates and dissociates as quickly as normal tubulin, but blocks subsequent addition of subunits, one might observe slower growth rates with qualitatively greater variability. We do not, however, believe that such tubulin could contribute substantially to the variability observed in these experiments. The protein was submitted to a fourth cycle of assembly/disassembly before the microscope experiment, and material from two separate preparations was examined with indistinguishable results. Because the hypothetical Tb* would have to be a reproducibly constant fraction of the total tubulin in solution after these manipulations and through multiple experiments and separate preparations, it is an unlikely causative agent.

### Simulations of microtubule dynamics

To address the difference between predicted ($Q = 1$) and experimental ($Q \approx 5$) variability, we used a model of

microtubule growth in which a Monte Carlo algorithm was used to add or remove subunits from the end of a 13-protofilament B-lattice microtubule. This model served to simulate growth and dynamics as a function of tubulin concentration and yielded dynamical parameters similar to the populations of microtubules monitored experimentally. Simulated microtubules displayed variability in growth rates, and their intrinsic variability was independent of growth rate with a similar average value ($6.8 \pm 0.6\ s^{-1}$) to that found for microtubules monitored experimentally. This indicates that in microtubule populations that exhibit dynamic behavior, including catastrophes and rescues, there is greater variability than the value of 1 expected from a simple model of subunit addition and loss from the end of a polymer.

Growth rates and variability in growth rates were determined for simulated microtubules by exactly the same method as microtubules observed with video-enhanced differential interference contrast microscopy as described in Material and Methods (Gamblin et al., 1996). The sampling rate and averaging window for computer-simulated microtubules was matched to that used for experimentally monitored microtubules. This allowed direct comparison of the growth rate and variability of computer-simulated and experimentally monitored microtubules. The lattice type and the mole fraction of GTP-Tb monomers (100%) in solution were fixed during the simulations. Observation of variability in growth rates in simulated microtubules is in apparent contrast to a report from Martin et al. (1993). The details of how growth rates were determined for simulated microtubules were not reported by Martin et al. (1993); however, averaging of growth rates over regions with long growth excursions may lead to the apparent discrepancy. We see no sustained regions of different growth rates for simulated microtubules that are characteristic of experimentally monitored microtubules.

A great advantage of computer simulations is that they can be used to simulate in vitro behavior without complications from experimental variables that present an unknown influence over observed behavior. In these simulations, there is significant intrinsic variability even though the lattice is defined and does not allow for any changes in protofilament number, incomplete hydrolysis of GTP, missing subunits within protofilaments, or lateral displacement between protofilaments. In addition, there are no complicating issues such as possible measurement errors or trivial experimental factors that could amplify any intrinsic variability in the rate of growth or shortening. The fact that the simulations presented here adequately mimic the experimental results demonstrates that dynamics and variability in growth rates occur in the absence of any complex or unpredictable factors.

The simulations presented in this paper allow us to address the issue of a possible correlation between the geometry of the microtubule end and the variability in the rate of growth. Chrétien et al. (1995) used cryogenic electron microscopy to study the complexity of the end of microtubules under known growth conditions. They found that the end of depolymerizing microtubules was generally blunt, and the length of the extension or irregularity of the end of growing microtubules was proportional to the rate of growth. Those findings are in contrast to studies by Simon and Salmon (1990), in which blunt ends were generally observed in micrographs of negatively stained microtubules that were fixed under conditions that favored growth. Our data revealed no evidence of a correlation between the roughness, or irregularity, of the microtubule end and the rate of growth (not shown). Thus, more irregularity in the microtubule end did not lead to more variable growth in our simulations.

Our model for simulating microtubule dynamics does not attempt to mimic the geometrical and associative complexities at the end of a growing or shortening microtubule. Microtubule dynamics in vivo and in vitro are certainly more complex than the process modeled in our simulations. In vitro studies have shown that in shortening microtubules, longitudinal interactions (intra-protofilament) persist even after lateral interactions are lost (Tran et al., 1997a), such that the subunits are lost in groups rather than as individuals. Our model does not address these geometrical complexities or dynamics at the minus end or have any provision for possible intermediate states (Tran et al., 1997b; Odde et al., 1995, 1996).

In summary, studies reported previously have ruled out several possible causes of variability in growth and shortening rates. It does not appear to result from impurities in solution, from exhaustion of GTP, from denaturation of tubulin, or from the presence of long-lived irregularities in the microtubule lattice (Gildersleeve et al., 1992). It is not due to the presence of trace amounts of microtubule-associated proteins (Billger and Williams, 1996). It is not due to fluctuations in the concentration of tubulin monomers due to slow diffusion in solution (Odde, 1997). The current data argue strongly that it is also not caused by irregularities incorporated into the tubulin lattice or by the presence of unsuspected subpopulations of microtubules. It therefore probably results from structural changes that are transient in time and associated with the dynamics of the growing and shortening end. This conclusion has been suggested by several other groups (Odde, 1997, 1996; Martin et al., 1993).

We thank T. Chris Gamblin and Marie-France Carlier for helpful discussions.

This work was supported by grant GM 25638 from the National Institutes of Health and by the Vanderbilt University Research Council.

## REFERENCES

Banerjee, A., and R. F. Ludueña. 1992. Kinetics of colchicine binding to purified beta-tubulin isotypes from bovine brain. *J. Biol. Chem.* 267: 13335–13339.

Banerjee, A., M. C. Roach, P. Trcka, and R. F. Ludueña. 1992. Preparation of a monoclonal antibody specific for the class IV isotype of beta-tubulin: purification and assembly of $\alpha\beta$II, $\alpha\beta$III, and $\alpha\beta$IV tubulin dimers from bovine brain. *J. Biol. Chem.* 267:5625–5630.

Bayley, P. M., M. J. Schilstra, and S. R. Martin. 1990. Microtubule dynamic instability: numerical simulation of microtubule transition properties using a lateral cap model. *J. Cell Sci.* 95:33–48.

Bayley, P. M., K. K. Sharma, and S. R. Martin. 1994. Microtubule dynamics in vitro. *In* Microtubules. J. S. Hyams and C. W. Lloyd, editors. Wiley-Liss, New York. 111–137.

Billger, M. A., G. Bhatacharjee, and R. C. Williams, Jr. 1996. Dynamic instability of microtubules assembled from microtubule- associated protein-free tubulin: neither variability of growth and shortening rates nor "rescue" requires microtubule-associated proteins. *Biochemistry.* 35: 13656–13663.

Billger, M., M. Wallin, R. C. Williams, Jr., and H. W. Detrich III. 1994. Dynamic instability of microtubules from cold-living fishes. *Cell. Motil. Cytoskel.* 28:327–332.

Bradford, M. M. 1976. A rapid and sensitive method for the quantitation of microgram quantities of protein utilizing the principle of protein-dye binding. *Anal. Biochem.* 72:248–254.

Bré, M. H., and E. Karsenti. 1990. Effects of brain microtubule-associated proteins on microtubule dynamics and the nucleating activity of centrosomes. *Cell. Motil. Cytoskel.* 15:88–98.

Carlier, M. F., and D. Pantaloni. 1981. Kinetic analysis of guanosine 5′-triphosphate hydrolysis associated with tubulin polymerization. *Biochemistry.* 20:1918–1924.

Chrétien, D., and S. D. Fuller. 2000. Microtubules switch occasionally into unfavorable configurations during elongation *J. Mol. Biol.* 298: 663–676.

Chrétien, D., S. D. Fuller, and E. Karsenti. 1995. Structure of growing microtubule ends: two-dimensional sheets close into tubes at variable rates. *J. Cell Biol.* 129:1311–1328.

Chrétien, D., F. Metoz, F. Verde, E. Karsenti, and R. H. Wade. 1992. Lattice defects in microtubules: protofilament numbers vary within individual microtubules. *J. Cell Biol.* 117:1031–1040.

Correia, J. J., L. T. Baty, and R. C. Williams, Jr. 1987. $Mg^{2+}$ dependence of guanine nucleotide binding to tubulin. *J. Biol. Chem.* 262: 17278–17284.

Correia, J. J., and S. Lobert. 2001. Physiochemical aspects of tubulin-interacting antimitotic drugs. *Curr. Pharm. Design.* 7:1213–1228.

Derry, W. B., L. Wilson, I. A. Khan, R. F. Ludueña, and M. A. Jordan. 1997. Taxol differentially modulates the dynamics of microtubules assembled from unfractionated and purified $\beta$-tubulin isotypes. *Biochemistry.* 36:3554–3562.

Detrich, H. W. III, and R. C. Williams. 1978. Reversible dissociation of the $\alpha\beta$ dimer of tubulin from bovine brain. *Biochemistry.* 17:3900–3907.

Dhamodharan, R., and P. Wadsworth. 1995. Modulation of microtubule dynamic instability in vivo by brain microtubule associated proteins. *J. Cell Sci.* 108:1679–1689.

Drechsel, D. N., A. A. Hyman, M. H. Cobb, and M. W. Kirschner. 1992. Modulation of the dynamic instability of tubulin assembly by the microtubule-associated protein tau. *Mol. Biol. Cell.* 3:1141–1154.

Drubin, D. G., and M. W. Kirschner. 1986. Tau protein function in living cells. *J. Cell Biol.* 103:2739–2746.

Dye, R. B., and R. C. Williams, Jr. 1996. Assembly of microtubules from tubulin bearing the nonhydrolyzable guanosine triphosphate analogue GMPPCP [guanylyl 5′-($\beta,\gamma$-methylenediphosphonate)]: variability of growth rates and the hydrolysis of GTP. *Biochemistry.* 35:14331–14339.

Erickson, H. P., and E. T. O'Brien. 1992. Microtubule dynamic instability and GTP hydrolysis. *Annu. Rev. Biophys. Biomol. Struct.* 21:145–166.

Gamblin, T. C., and R. C. Williams, Jr. 1995. Determination of microtubule polarity in vitro by the use of video-enhanced differential-interference contrast light microscopy and *Chlamydomonas* flagellar axonemal pieces. *Anal. Biochem.* 232:43–46.

Gamblin, T. C., K. Nachmanoff, S. Halpain, and R. C. Williams, Jr. 1996. Recombinant microtubule-associated protein 2c reduces the dynamic instability of individual microtubules. *Biochemistry.* 35:12576–12586.

Gildersleeve, R. F., A. R. Cross, K. E. Cullen, A. P. Fagen, and R. C. Williams, Jr. 1992. Microtubules grow and shorten at intrinsically variable rates. *J. Biol. Chem.* 267:7995–8006.

Goode, B. L., P. E. Denis, D. Panda, M. J. Radeke, H. P. Miller, L. Wilson, and S. C. Feinstein. 1997. Functional interactions between the proline-rich and repeat regions of tau enhance microtubule binding and assembly. *Mol. Biol. Cell.* 8:353–365.

Horio, T., and H. Hotani. 1986. Visualization of the dynamic instability of individual microtubules by dark-field microscopy. *Nature.* 321: 605–607.

Hoyle, H. D., and E. C. Raff. 1990. Two *Drosophila* $\beta$-tubulin isoforms are not functionally equivalent. *J. Cell Biol.* 111:1009–1026.

Hutchens, J. A., H. D. Hoyle, F. R. Turner, and E. C. Raff. 1997. Structurally similar *Drosophila* $\alpha$-tubulins are functionally distinct in vivo. *Mol. Biol. Cell.* 8:481–500.

Kowalski, R. J., and R. C. Williams, Jr. 1993a. Unambiguous classification of microtubule-ends in vitro: dynamic properties of the plus- and minus-ends. *Cell. Motil. Cytoskel.* 26:282–290.

Kowalski, R. J., and R. C. Williams, Jr. 1993b. Microtubule-associated protein 2 alters the dynamic properties of microtubule assembly and disassembly. *J. Biol. Chem.* 268:9847–9855.

Ludueña, R. F. 1998. Multiple forms of tubulin: different gene products and covalent modifications. *Int. Rev. Cytol.* 178:207–275.

Mandelkow, E. M., E. Mandelkow, and R. A. Milligan. 1991. Microtubule dynamics and microtubule caps: a time-resolved cryo-electron microscopy study. *J. Cell Biol.* 114(5):977–991.

Martin, S. R., M. J. Schilstra, and P. M. Bayley. 1993. Dynamic instability of microtubules: Monte Carlo simulation and application to different types of microtubule lattice. *Biophys. J.* 65:578–596.

Melki, R., S. Fievez, and M. F. Carlier. 1996. Continuous monitoring of $P_i$ release following nucleotide hydrolysis in actin or tubulin assembly using 2-amino-6-mercapto-7-methylpurine ribonucleoside and purine-nucleoside phosphorylase as an enzyme-linked assay. *Biochemistry.* 35:12038–12045.

Mitchison, T., and M. Kirschner. 1984. Dynamic instability of microtubule growth. *Nature.* 312:237–242.

Morrison, N. 1969. Introduction to Sequential Smoothing and Prediction. McGraw Hill, New York. 246–247.

Odde, D. J. 1997. Estimation of the diffusion-limited rate of microtubule assembly. *Biophys. J.* 73:88–96.

Odde, D. J., L. Cassimeris, and H. M. Buettner. 1995. Kinetics of microtubule catastrophe assessed by probabilistic analysis. *Biophys. J.* 69: 796–802.

Odde, D. J., L. Cassimeris, and H. M. Buettner. 1996. Spectral analysis of microtubule assembly dynamics. *Am. Inst. Chem. Eng.* 42:1434–1442.

Oosawa, F. 1970. Size distribution of protein polymers. *J. Theor. Biol.* 27:69–86.

Panda, D., B. L. Goode, S. C. Feinstein, and L. Wilson. 1995. Kinetic stabilization of microtubule dynamics at steady state by tau and microtubule-binding domains of tau. *Biochemistry.* 34:11117–11127.

Panda, D., H. P. Miller, A. Banerjee, and L. Wilson. 1994. Microtubule dynamics in vitro are regulated by the tubulin isotype composition. *Proc. Natl. Acad. Sci. U.S.A.* 91:11358–11362.

Pierson, G. B., P. R. Burton, and R. H. Himes. 1978. Alterations in number of protofilaments in microtubules assembled in vitro *J. Cell Biol.* 76: 223–228.

Pryer, N. K., R. A. Walker, V. P. Skeen, B. D. Bourns, M. F. Soboeiro, and E. D. Salmon. 1992. Brain microtubule-associated proteins modulate microtubule dynamic instability in vitro: real-time observations using video microscopy. *J. Cell Sci.* 103:965–976.

Rodionov, V. I., and G. G. Borisy. 1997. Microtubule treadmilling in vivo. *Science.* 275:215–218.

Schnapp, B. J. 1986. Viewing single microtubules by video light microscopy. *Methods Enzymol.* 134:561–573.

Shelden, E., and P. Wadsworth. 1993. Observation and quantification of individual microtubule behavior in vivo: microtubule dynamics are cell-type specific. *J. Cell Biol.* 120:935–945.

Simon, J. R., and E. D. Salmon. 1990. The structure of microtubule ends during the elongation and shortening phases of dynamic instability examined by negative-stain electron microscopy. *J. Cell Sci.* 96: 571–582.

Tran, P. T., P. Joshi, and E. D. Salmon. 1997a. How tubulin subunits are lost from the shortening ends of microtubules. *J. Struct. Biol.* 118: 107–118.

Tran, P. T., R. A. Walker, and E. D. Salmon. 1997b. A metastable intermediate state of microtubule dynamic instability that differs significantly between plus and minus ends. *J. Cell Biol.* 138:105–117.

Walker, R. A., E. T. O'Brien, N. K. Pryer, M. F. Soboeiro, W. A. Voter, H. P. Erickson, and E. D. Salmon. 1988. Dynamic instability of individual microtubules analyzed by video light microscopy: rate constants and transition frequencies. *J. Cell Biol.* 107:1437–1448.

Williams, R. C., Jr., and J. C. Lee. 1982. Preparation of tubulin from brain. *Methods Enzymol.* 85:376–385.

Williams, R. C., Jr. 1992. Analysis of microtubule dynamics in vitro. *In* The Cytoskeleton: A Practical Approach. K. L. Carraway, editor. Oxford University Press, Oxford. 151–166.

Wilson, P. G., and G. G. Borisy. 1997. Evolution of the multi-tubulin hypothesis *Bioessays.* 19:451–454.

Witman, G. B. 1986. Isolation of *Chlamydomonas* flagella and flagellar axonemes. *Methods Enzymol.* 134:280–90.